Journal of Inclusion Phenomena and Macrocyclic Chemistry (2024) 104:83–98
https://doi.org/10.1007/s10847-024-01219-3

ORIGINAL ARTICLE

Chiral recognition of fenchone and camphor by α-CD through the multi-equilibrium GFN2-xTB quantum approach

Cleber Paulo Andrada Anconi[1]

Received: 31 August 2023 / Accepted: 11 January 2024 / Published online: 17 February 2024

Abstract

Binding constants for host-guest cyclodextrin systems have been estimated recently through the small-cost GFN2-xTB semiempirical quantum method in a multi-equilibrium scope. This work applied such an approach to investigate the inclusion of fenchone and camphor into α-cyclodextrin. The computational cost associated with GFN2-xTB and the supramolecular arrangements automated obtained by UD-APARM allowed the investigation of an unprecedented 18,615 starting systems (8640 for 1:1 guest/CD and 5184 + 2232 + 2559 for 1:2 guest/CD stoichiometry). According to the present study, only 18 (0.21%) for 1:1 associations and 45 (0.45%) for 1:2 associations contribute to the binding constants. The chiral recognition was achieved for the four inclusion compounds investigated: (−)-fenchone@$(\alpha\text{-CD})_2$, (+)-fenchone@$(\alpha\text{-CD})_2$, and (−)-camphor@$(\alpha\text{-CD})_2$ and (+)-camphor@$(\alpha\text{-CD})_2$. When experimental and theoretical GFN2-xTB (ALPB) binding constants were compared, a linear correlation with an R^2 equal to 0.9933 was obtained. Estimated error varied from 1 to 3% to adjusted GFN2-xTB values. Furthermore, the theoretical data supported the experimental information that two CD units encapsulate camphor guests, increasing their stabilities. The procedure adopted can be expanded to investigate other 1:1 and 1:2 chiral host-guest systems for which it was addressed that finding out representative host-guest systems correspond to the bottleneck in the use of the discussed GFN2-xTB/UD-APARM multi-equilibrium approach.

✉ Cleber Paulo Andrada Anconi
cleberanconi@ufla.br

[1] Institute of Natural Sciences, Department of Chemistry, Federal University of Lavras, Lavras 37200-900, Brazil

Graphical abstract

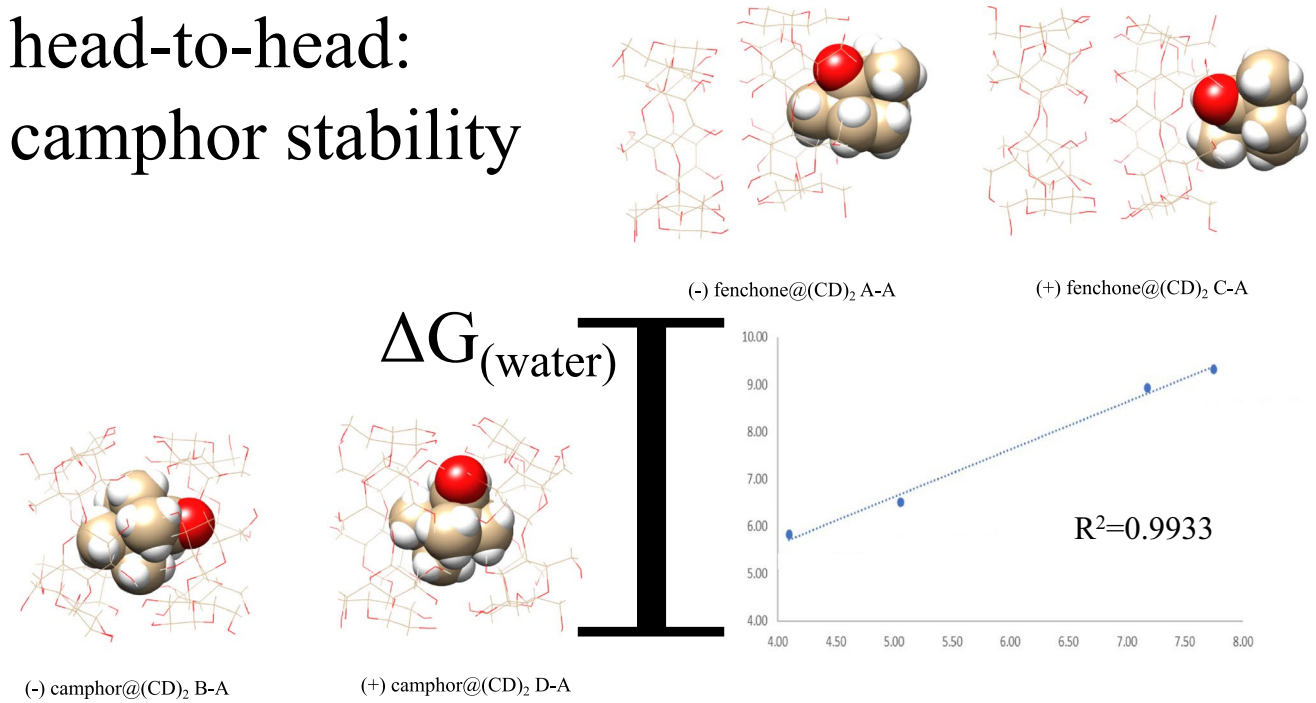

Keywords Cyclodextrin · Chiral recognition · GFN2-xTB · UD-APARM

Introduction

Cyclodextrins (CDs) comprise a class of compounds that form favorable supramolecular systems with a wide range of substances [1–3]. The applicability of such a carbohydrate is related to the accommodation in the CD cavity of a guest molecule to form an inclusion compound. The applications of such a type of compound, also named host-guest system, vary from food science [4] to pharmaceutics [5], being also relevant in the development of remediation technologies [6–9]. Chiral recognition is essential in life sciences and relevant to Chemistry, specifically focusing on separation techniques [10]. The chiral nature of CDs extends their applicability [11, 12]. Since CDs are chiral compounds, they can act as receptors to bind distinct molecules, as addressed experimentally, for which the binding constant can be determined [13]. One fundamental aspect of chiral recognition by CDs is related to the difference in the spatial accommodation of one specific enantiomer on the CD cavity. How far the chirality center is located concerning the accommodation of a given guest inside the CD cavity plays a crucial role in chiral separation. For instance, the distance of the chirality center concerning the CD cavity accounts for the incapacity of β-CD to resolve warfarin enantiomers in contrast to the excellent resolution for mephobarbital [14]. Other critical experimental information concerns the binding constants for R and S enantiomers acting as guests in a CD-based host-guest system. The values for such binding constants can be very close [12, 15], increasing the challenge of using theoretical methods to investigate chiral recognition.

With a focus on theoretical methodology, one significant challenge is finding the proper balance between the accuracy required to differentiate small binding constants of including chiral guests into CDs and the computational cost of the chosen method. Predicting the formation of host-guest systems corresponds to one fundamental goal attributed to using a theoretical formalism to treat CD systems. Since host-guest systems are flexible, many arrangements must be investigated. Exploring the Potential Surface Energy (PES) of a given method corresponds to a bottleneck to applying the theoretical methodology, particularly for approaches based on quantum mechanics. Due to the enormous number of systems to be modeled, treating CD chiral recognition with sophisticated quantum approaches is prohibitive. In this context, quantum semiempirical methodologies seem to be a natural choice. However, not all available semiempirical methods can be employed to study CD-based systems [16].

Grimme et al. recently developed the GFN2-xTB method [17, 18], a low-cost semiempirical quantum approach that has shown reliable applicability to study CD-based systems

[19, 20]. Applying the GFN2-xTB to CD-based systems involves investigating many supramolecular starting arrangements. Recently, using axes of inertia, an alternative form to characterize and obtain the Cartesian coordinates of a supramolecular system, was addressed [21]. The software related to such a contribution, the UD-APARM, produces hundreds or thousands of starting supramolecular systems on an automated and reproducible basis. Recently, systems obtained through the UD-APARM were investigated with the GFN2-xTB method in a multi-equilibrium approach to obtain reliable CD-based binding constants [22, 23]. The promisor outcomes obtained serve as motivation to test the methodology for chiral recognition for CD-based host-guest systems.

Within the present work, the chiral recognition of the camphor and fenchone enantiomers by α-CD was investigated by applying the semiempirical GFN2-xTB method with the aid of the UD-APARM software in a multi-equilibrium scope. The relatively small computational cost of the GFN2-xTB implementation in association with an automated procedure to obtain the spatial Cartesian coordination through UD-APARM allowed the investigation of an unprecedented 18,615 starting systems for fenchone and camphor enantiomers (8640 for 1:1 guest/CD; 5184 for 1:2 guest/CD stoichiometry, and additional 2232 (3 × 744) and 2559 (3 × 853) for 1:2 (+)-camphor/α-CD systems). The slight differences in the binding constants for the complexation of such bicyclic terpenoid enantiomers into α-CD, the massive number of starting systems required to obtain reliable data, and the approach's limitations are discussed within the present contribution that enhances the challenge of modeling such type of systems.

Methods

Isolated camphor and fenchone molecules were obtained from PubChem [24] with the following identifiers: (1R,4R) (+)-camphor (PubChem identifier: CID 159,055); (1 S, 4 S) (−)-camphor (PubChem identifier: CID 444,294); (1R,4 S) (−)-fenchone (PubChem identifier: CID 82,229); (1 S,4R) (+)-fenchone (PubChem identifier: CID 1,201,521). The α-CD structure was obtained from X-ray [25] without water molecules. The structure of all compounds studied herein is shown in Fig. 1.

The GFN2-xTB method [18, 26] was employed to optimize the isolated starting structures obtained from PubChem (camphor and fenchone) and X-ray crystallography (α-CD). The ALPB continuum approach [27] was employed to study the system in aqueous media. The UD-APARM software [21] (https://github.com/anconi-lab) was used to obtain starting geometries. All systems were optimized with the GFN2-xTB method at vacuum and subsequently within a continuum solvent approach for water at 300.6 K, the experimental condition [28, 29].

The camphor and fenchone compounds (Fig. 1) investigated within this theoretical chiral study were chosen because of their small conformational degrees of freedom. As we can see from Fig. 1, their structures are rigid. With rigid guests, one can focus on the applicability of the

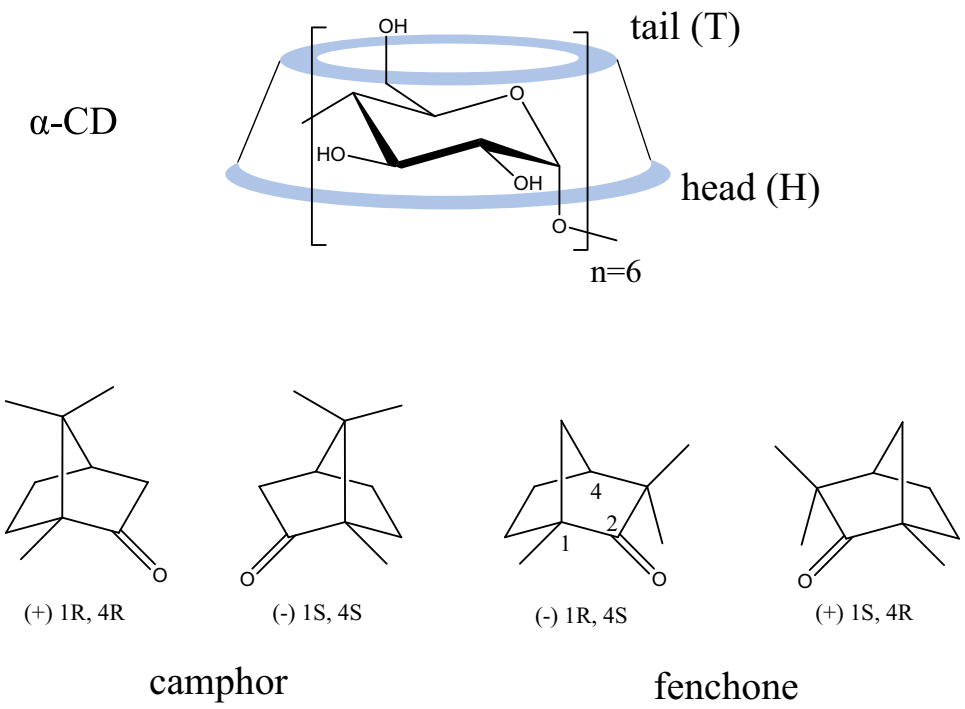

Fig. 1 Host (α-CD) and guests (camphor and fenchone) studied herein. For the CD, the identification of the rims as head (H) and tail (T) comprising secondary and primary hydroxyl groups, respectively, is shown

recently developed GFN2-xTB multi-equilibrium approach with less influence on the conformational study. The host (α-CD) and the camphor (+), camphor (−), fenchone (+), and fenchone (−) were submitted to the UD-APARM for the construction of 1:1 supramolecular associations.

The essential idea implemented in UD-APARM and discussed in ACS Omega [21] concerns establishing the relative position and rotation of the entities of a supramolecular association through constructing a Cartesian reference system over the axes of inertia of one molecule. It is worth noting that only the evaluation of the principal axis of inertia does not allow the construction of the Cartesian system because no preferential direction can be attributed. For this task, the center of mass of the set of atoms with the higher atomic number (oxygen for CDs) is employed as a reference. Modifications in the UD-APARM software were implemented to determine the Cartesian axis over the center of mass of the supramolecular systems formed with two CD units, such as the head-to-head (HH) association. Within the present work, for 1:1 (+) fenchone/α-CD, (−) fenchone/α-CD, (+) camphor/α-CD, (−) camphor/α-CD, UD-APARM software constructed 2160 supramolecular arrangements with the parameters given in Table S1.

According to Table S1, 8,640 1:1 starting systems (4 × 2160) were investigated at the GFN2-xTB level of theory. For the 1:2 guest/CD systems, the starting orientation with Euler rotational angles corresponding to zero gives rise to a system with a perpendicular spatial arrangement, as shown in Fig. 2 (marked in red). As we expect the interaction between the CD rims, the β Euler fixed at 90 degrees allows the CDs to face each other (as shown in Fig. 2, right). In such conditions, the γ Euler angle will vary instead of the α Euler angle to produce distinct supramolecular 1:2 guest/CD arrangements with the CD unit fixed in space interacting with the guest/CD pair (upper in Fig. 2) with distinct rotational orientation along the CD axis of inclusion.

The 1:2 guest/CD arrangements were obtained with the most favorable 1:1 optimized systems. For each guest/CD pair, 288 starting arrangements were constructed with UD-APARM with the ranges in Table S2. As eighteen 1:1 stable inclusion compounds were identified: four (+)-fenchone/α-CD, one (−)-fenchone/α-CD, five (+)-camphor/α-CD, and eight (−)-camphor/α-CD, 5,184 1:2 guest/CD systems (18 × 288) were investigated at GFN2-xTB level of theory.

After the first analysis, additional optimizations were carried out for three specific types of associations for (+) camphor and α-CD to investigate new 1:2 stable arrangements. Each new PES investigation comprised 744 optimizations for 1:2 systems with input described in Table S3. For the 1:2 associations, 5184 + 2232 (3 × 744) and, therefore, 7416 systems were investigated (fully optimized with harmonic frequency evaluation) at the GFN2-xTB (ALPB) level of theory. Finally, after modifying the UD-APARM to account for supramolecular systems with some symmetry, such as HH CD-based associations, additional calculations were carried out for camphor(+)@$(\alpha\text{-CD})_2$ systems according to Table S4 (totaling 2559 additional calculations, 3 × 853).

This work adopted the multi-equilibrium approach, and Gibb energy in solution is computed as previously addressed [22]. For the present work, the binding constants were evaluated at T = 300.6 K, the temperature of the experiments [28, 29]. The formations of 1:1 and 1:2 guest (g)/host (CD) compounds were studied according to Eqs. (1) and (3). Equations (4) and (5) define the sequential macroscopic binding

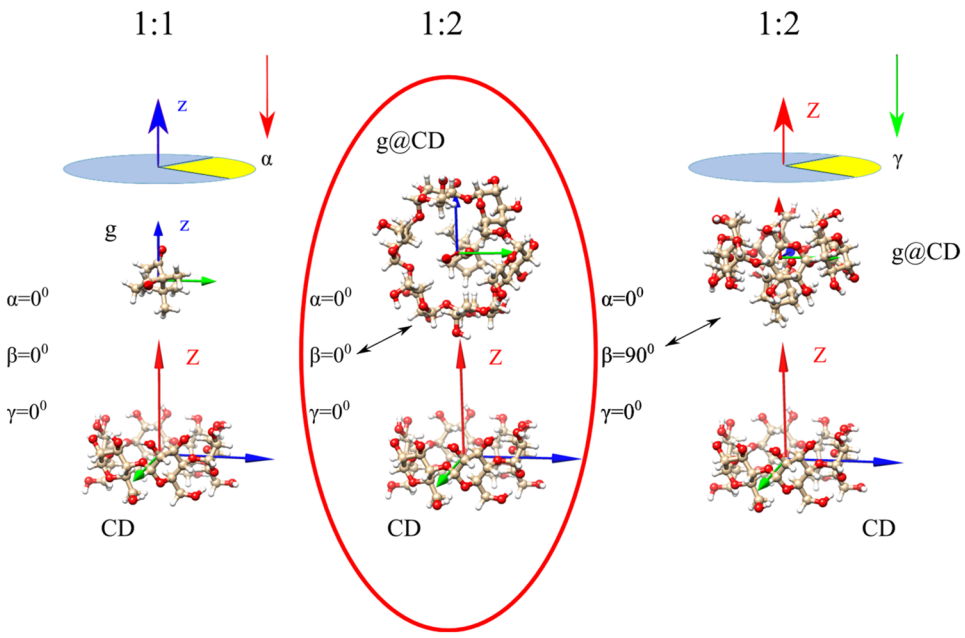

Fig. 2 For the 1:2 guest/CD systems investigated herein, null Euler rotational angles (α = β = γ = 0 degrees) correspond to a perpendicular spatial arrangement (marked in red). For 1:1 (left), the starting null Euler rotational angles correspond to the natural initial guest orientation. With a β Euler angle equal to 90 degrees or 1:2 guest/CD systems, both CD units (formed by the reference and the g@CD) face each other to interact (right). In such a spatial arrangement, the γ Euler angle accounts for the rotation of the upper system to form the possible 1:2 guest/CD arrangements (right)

constants (K_1 and K_2) with square brackets denoting molar concentrations in which [g] corresponds to the molar concentration for the guest, [CD] the molar concentration of the α-CD, [g@CD] the molar concentration of a 1:1 host-guest system, and [g@$(CD)_2$] the molar concentration of the 1:2 guest/CD system. Beyond the sequential macroscopic binding constants, Eq. (6) defines the overall association constant [28], also named the overall binding constant, β_{12}, the quantity computed at the GFN2-xTB (ALPB) level of theory for comparison to experimental data for 1:2 guest/CD systems. According to (3), $\beta_{12} = K_1 . K_2$. For the theoretical evaluation of Gibbs energy, within this work, Eqs. (1) and (2) were used for 1:1 and 1:2 inclusion formation, respectively.

$$g + CD \rightleftharpoons g@CD, \tag{1}$$

$$g@CD + CD \rightleftharpoons g@(CD)_2, \tag{2}$$

$$g + 2CD \rightleftharpoons g@(CD)_2, \tag{3}$$

$$K_1 = \left[\mathrm{g@CD}\right] / \left[\mathrm{g}\right]\left[\mathrm{CD}\right], \tag{4}$$

$$K_2 = \left[\mathrm{g@}(CD)_2\right] / \left[\mathrm{g@CD}\right]\left[\mathrm{CD}\right], \tag{5}$$

$$\beta_{12} = \left[\mathrm{g@}(CD)_2\right] / \left[\mathrm{g}\right][CD]^2. \tag{6}$$

After optimization and frequency evaluation in the gas phase and re-optimization in the continuum model, the representative systems were submitted to the APARM software to compute the association parameters and check the integrity of the supramolecular systems. Gibbs energy of formation was computed for 1:1 and 1:2 guest/CD pairs with Eqs. (7) and (8), respectively, in which ΔG^0 corresponds to gas phase Gibbs energy, at 300.6 K. Gibbs energy of formation in solution was evaluated with Eq. 9 as previously discussed [22, 23].

$$\Delta G^0 = G^0(g@CD) - G^0(g) - G^0(CD), \tag{7}$$

$$\Delta G^0 = G^0[g@(CD)_2] - G^0(g) - 2G^0(CD), \tag{8}$$

$$\Delta G_{water} = \Delta G^0 + \delta \Delta G_{solv}. \tag{9}$$

The studied systems were used to obtain the theoretical binding constant from the most stable (the reference) until they achieved a difference from the reference corresponding to 3.0 kcal mol^{-1}. Such systems were analyzed by APARM software to obtain the association parameters and check the integrity of the optimized geometries. The 3.0 kcal mol^{-1} window limits the number of systems to be considered for computing the theoretical binding constants. Differences greater than 3.0 kcal mol^{-1} implied a negligible contribution to the evaluation of K. The Gibbs energy of formation was computed with Eqs. 8 and 9, and the theoretical binding constant was obtained with the summation of individual binding constants, as discussed previously [22].

Some representative supramolecular systems were investigated with the B97-D functional [30], using the SMD [31] continuum approach, as implemented in the ORCA package [32]. The version of ORCA used corresponds to the 5.0.1. The CREST (Conformer-Rotamer Ensemble Sampling Tool) [33] was also used to treat some supramolecular representative systems.

UD-APARM and APARM, along with instructions, are free and available for download at https://github.com/anconi-lab. All isolated and 1:1 stable guest@CD systems Cartesian coordinates required to reproduce the entire study were included in the supplementary information file, along with instructions employed in the calculations. The supporting information file describes further information concerning the procedure adopted in this contribution.

Results and discussion

The Potential Energy Surface (PES) exploration at the GFN2-xTB level of theory was carried out within this work for each guest/CD pair with the aid of the UD-APARM software. The starting investigation concerned the 1:1 guest/CD pairs. From the investigation of 8640 1:1 supramolecular associations, only 37 (0.43%) present $\Delta G_{water} < 0$, being 18 (0.21%) distinct or non-equivalent supramolecular systems. CD-based systems with $\Delta G_{water} < 0$ are not representative and must be avoided, as discussed previously [22]. After the xTB (ALPB) optimization stage, the APARM software was used to distinguish the inclusion compounds under investigation. The APARM data and Gibbs energies in solution computed with Eqs. 7 and 9 were included in Table 1 for the 1:1 systems under study.

From Table 1, it can be stated that a variety of inclusion systems were found in which no regular pattern concerning the association parameters (r, θ, α, β, and γ) can be addressed. It is noticeable that the distance of the center of mass between the host and guest does not correspond to zero or some value close to such a small distance, and the r parameter varies from 3.1 to 5.0 Å.

For clarity, the spatial arrangement can be analyzed with the simple representation of gT or gH. An individual CD molecule possesses a cavity with two rims, one comprising the secondary hydroxyl groups identified as head (H) and another rim with primary hydroxyl groups identified as tail (T), as illustrated in Fig. 1. Such notation is essential in the investigation of CD associations in which we have the following possible associations: HH, HT, and TT [34, 35].

Table 1 Association free energies (ΔG_{water}) in continuum ALPB model, computed with Eqs. 7 and 9, and the corresponding supramolecular main parameters (APARM data) for relative position (r, θ) and relative rotation (α, β, and γ)

Compound	log K_1 (xTB)	ID	Spatial representation	ΔG_{water} (kcal mol^{-1})	r (Å)	θ (deg)	α (deg)	β (deg)	γ (deg)
(+) fenchone@α-CD	0.90	A	gT	− 0.62	4.3	177	272	212	310
		B	gH	− 0.58	3.6	10	1	206	87
		C	gT	− 0.23	5.0	172	60	53	312
		D	gH	− 0.06	3.4	11	307	136	345
(−) fenchone@α- CD	0.23	A	gT	− 0.32	4.2	171	94	33	40
(+) camphor@α- CD	1.42	A	gH	− 1.46	3.1	5	326	209	303
		B	gT	− 1.15	5.3	176	279	329	305
		C	gT	− 0.89	4.6	176	105	330	25
		D	gH	− 0.45	3.2	7	232	261	57
		E	gH	− 0.27	3.9	12	26	267	73
(−) camphor@α- CD	2.02	A	gT	− 2.34	5.0	178	194	34	349
		B	gH	− 1.99	3.2	4	193	203	353
		C	gT	− 1.25	4.7	175	224	313	56
		D	gT	− 1.18	5.0	173	157	82	47
		E	gH	− 0.98	3.1	1	34	151	89
		F	gH	− 0.81	3.6	11	160	271	58
		G	gT	− 0.40	4.2	175	35	316	76
		H	gT	− 0.29	4.9	173	69	23	37

The data was collected from the representative 1:1 systems (0.21% of the 8640) used to obtain the binding constants at the GFN2-xTB (ALPB) level of theory at 300.6 K

The spatial arrangement of a guest (g) pointing toward the tail (T) portion of the CD is identified with gT, and pointing toward the head (H) portion of the CD is identified as gH.

With a focus on the position of the guest in the 1:1 inclusion compounds, we see from Table 1 that the polar angle θ close to 180 degrees implies the guest (g) pointing toward the tail (T) portion of the CD (gT compounds) and θ close to 0 degrees implies the guest (g) pointing toward head (H) portion of the CD (gH compounds). Some representative optimized associations for 1:1 (+) fenchone@α-CD, (−) fenchone@α-CD, (+) camphor@α-CD, and (−) camphor@α-CD are depicted in Fig. 3.

Table 1 also shows the Gibbs energies of formation in water (ΔG_{water}) for fenchone and camphor inclusion into α-CD. According to GFN2-xTB (ALPB) data, for 1:1 systems, including camphor into α-CD is more favorable than fenchone due to the values log K_1. The most negative values of Gibbs energy of inclusion also attest to such a trend.

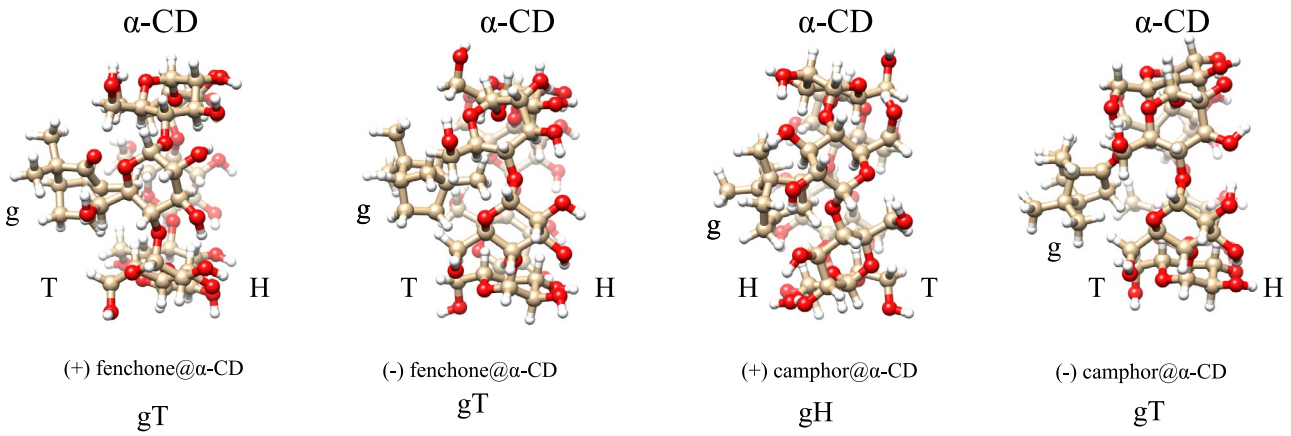

Fig. 3 Spatial arrangements of the most stable 1:1 host-guest systems optimized at GFN2-xTB (ALPB) level of theory (A systems in Table 3). The identification of the guest spatial orientation concerning the CD cavity (gT or gH) is also indicated

Interestingly, experimental contributions did not address K_1 for camphor inclusion into α-CD [28, 36, 37]. According to Table 1, the binding constants for including camphor into α-CD are higher than those computed for including fenchone.

Each system identified for the capital letters in Table 1 was used as a starting arrangement to study the 1:2 guest/CD compounds. For each system, the association with another CD unit occurs according to the range of parameters in Table S2. The UD-APARM scan for the 1:2 association corresponds to the study of arrangements formed by the association of a 1:1 inclusion compound (each one in Table 1) and another CD unit. To approximate the inclusion compound from another CD unit used as a reference, the β Euler was kept at 90 degrees, as illustrated in Fig. 2. For the association of each system in Table 1 with another CD, 288 arrangements were investigated, totaling 5,184 (18 × 288) new GFN2-xTB optimizations with subsequent frequency evaluation in a vacuum with the corresponding optimization in the continuum solvation model (ALPB) for water. With the use of the initial scan for 1:2 guest/CD systems (Table S2 for UD-APARM input), the logarithm of the overall binding constant (log β_{12}) corresponding to 5.06, 4.10, 4.65, and 7.18 were computed at GFN2-xTB (ALPB) level of theory, in a multi-equilibrium scope, for (+) fenchone@$(CD)_2$, (−) fenchone@$(CD)_2$, (−) camphor@$(CD)_2$, and (−) camphor@$(CD)_2$, respectively.

The comparison to experimental information [29, 38] suggests an issue related to the data for (+) camphor@$(CD)_2$. The binding constant for such a system should be higher. According to our previous contribution [23], an additional scan is recommended to improve the theoretical association constant computed. With the analysis of the overall spatial arrangement (as will be discussed), a new scan was defined (Table S3). The new scan was applied to the formation of (+) camphor@$(CD)_2$ with the use of the association of 1:1 systems with gH arrangements (A, D, and E in Table 1). The scan in Table S3 implies an additional 744 systems for A, D, and E, which increased the total of arrangements investigated with another 2232 supramolecular associations. An improved log β_{12} corresponding to 5.65 was computed for (+) camphor@(α-$CD)_2$. The data obtained from the analysis of umprecedent 7416 (5184 + 2232) systems at GFN2-xTB (ALPB) level of theory for 1:2 guest/CD systems were included in Table 2. It is noticeable that in a 3.0 kcal mol^{-1} windown, 25 guest@$(CD)_2$ were identified, 0.34% of 7416 starting associations.

Since the 1:2 systems in Table 2 were obtained from the compounds listed in Table 1, the ID shown in Table 2 depends on the previous notation. For instance, in Table 1, only one 1:1 inclusion compound was found among 2160 starting systems for (−) fenchone@α-CD, and such a compound was identified with the capital letter A. After optimizing 288 new systems formed with such association and another CD unit, three stable compounds in water were found in a 3.0 kcal mol^{-1} window. Therefore, from the 1:1 A, the following 1:2 systems were identified: A-A, A-B, and A-C (see Table 2).

Not necessarily all combinations from Table 1 were included in Table 2 due to the Gibbs energy computed and the 3.0 kcal mol^{-1} window. We see from Table 2 only one ID (B-A) for (−) camphor@$(CD)_2$. Only the B-A system is listed for this host-guest compound because such a system corresponds to the most stable one, identified with $\Delta G_{water} = -9.87$ kcal mol^{-1}. Such a compound is at least 3.0 kcal mol^{-1} more stable than any other association of this guest included in $(CD)_2$. Interestingly, the order concerning the capital letters for 1:1 systems was not necessarily kept when 1:1 and 1:2 compounds were compared. We see from Table 2 that for (+) camphor@$(CD)_2$, the most stable association (for which $\Delta G_{water} = -7.05$ kcal mol^{-1}) was found for the combination of the D 1:1 inclusion compound in Table 1 with another CD unit. Within Table 2, such a 1:2 compound is identified as D-A.

The comparison between the Gibbs energies from Tables 1 and 2 indicates that the association with another CD unit to form a 1:2 guest/host system promotes a significant stabilization. The Gibbs energies of association (ΔG_{water}) became much more negative with the association of another CD.

Concerning the association parameters, the distances of the center of mass are considerably higher for 1:2 systems. We now have the distance between the center of mass of a CD unit and the inclusion compound used to form the 1:2 system. The overall spatial arrangement is also indicated in Table 2, and its relation to energy and the r parameter can be discussed. We see the predominance of a type of arrangement identified as g(HH) for fenchone@$(\alpha CD)_2$ compounds and HgH for camphor@(α-$CD)_2$ compounds. With a focus on the most stable compounds identified for each guest, we see the accordance between the GFN2-xTB (ALPB) data and experimental findings in which the most negative Gibbs energies and consequently higher log β_{12} are attributed to camphor@(α-$CD)_2$ systems [23].

For C-A of the (+) fenchone@$(\alpha CD)_2$, the first line in Table 2, we see the indication of $\Delta G_{water} = -6.83$ kcal mol^{-1} and $r = 7.8$ Å. Such an optimized arrangement is shown in Fig. 4. We see from Fig. 4 that both CD units interact, forming the HH (head-to-head) association between two CDs. The guest is not included between the two CD units. It is possible to argue that we have a guest interacting with the HH association (in general). Such a type of association was denoted g(HH), and many hydrogen bonds can be identified between the CD units (see Fig. 4). It is also possible to consider for this formation the following notation: gT + CD ⇌ g(HH). The g(HH) arrangement is the only

Table 2 Association free energies (ΔG_{water}) in continuum ALPB model, computed with Eq. (3) and the corresponding supramolecular main parameters (APARM data) for relative position (r, θ) and relative rotation (α, β, and γ). The data was collected from the representative 1:2 guest@CD systems (0.34% of 7416) used to obtain the binding constants at the GFN2-xTB (ALPB) level of theory at 300.6 K (within a 3.0 kcal mol^{-1} window)

Compound	log β_{12}	ID	Spatial representation	ΔG_{water} (kcal mol^{-1})	r (Å)	θ (deg)	α (deg)	β (deg)	γ (deg)
(+) fenchone@(α-CD)$_2$	5.06	C-A	g(HH)	− 6.83	7.8	17	3	268	273
		A-A	g(HH)	− 5.39	7.8	5	177	87	41
		E-A	g(HH)	− 5.14	8.0	157	189	270	297
		A-B	g(HH)	− 4.70	7.8	21	179	90	19
		A-C	g(HH)	− 4.46	7.9	4	182	88	334
		C-C	g(HH)	− 4.37	8.0	5	0	264	347
		A-D	g(HH)	− 4.07	7.9	4	182	88	350
		A-E	g(HH)	− 3.85	7.6	23	359	270	279
(−) fenchone@(α-CD)$_2$	4.10	A-A	g(HH)	− 5.52	7.7	13	358	269	316
		A-B	g(HH)	− 4.53	7.7	17	181	89	283
		A-C	g(HH)	− 3.45	7.9	7	2	269	335
(+) camphor@(α-CD)$_2$	5.65	D-A	HgH	− 7.05	6.8	4	184	272	66
		E-A	HgH	− 6.86	6.7	5	182	271	2
		A-A	HgH	− 6.78	6.4	1	182	270	61
		E-B	HgH	− 6.43	6.8	6	3	88	358
		E-C	HgH	− 6.31	6.8	5	183	271	36
		D-B	HgH	− 6.01	6.6	4	181	277	66
		D-C	HgH	− 5.17	6.8	5	4	88	64
		E-D	HgH	− 5.01	6.8	6	2	88	21
		A-B	g(TT)	− 4.83	8.8	177	332	88	301
		E-E	HgH	− 4.49	6.6	6	4	91	65
		D-E	HgH	− 4.31	6.8	5	176	270	49
		A-C	g(TH)	− 4.29	7.9	2	0	268	35
		E-F	HgH	− 4.17	6.7	8	176	267	26
(−) camphor@(α-CD)$_2$	7.18	B− A	HgH	− 9.87	6.4	2	183	271	76

The GFN2-xTB (ALPB) log β_{12} was computed in a multi-equilibrium approach

one identified for fenchone@$(CD)_2$, contributing to the β_{12} overall binding constant.

With a focus on camphor@$(CD)_2$, we see from Table 2 that the guest is accommodated inside a CD dimer for many representative systems. Such associations denoted by HgH are shown in Fig. 5. Many intermolecular hydrogen bonds are formed between the CDs in a head-to-head (HH) association that accommodates a camphor guest inside. Other arrangements were also identified, such as g(TH) and g(TT) (see Table 2). Besides the existence of g(HT) and g(TT), according to Table 2, the HgH arrangement is predominant for champhor@$(CD)_2$. Interestingly, the present theoretical study concerning the camphor inclusion into α-CD gives support at a molecular level for experimental conclusions [29] in which the 1:2 complex presents a strong predominance with the indication that camphor is embedded in an arrangement formed by two α-CD molecules.

With a focus on comparing theoretical GFN2-xTB (ALPB) and experimental binding constants, at this stage of the analysis, an opposite trend concerning the inclusion into α-CD was identified for camphor isomers. At this stage, the GFN2-xTB (ALPB) log β_{12} correspond to 5.65 and 7.18 for (+) camphor@(α-CD)$_2$ and (−) camphor@(α-CD)$_2$, respectively. The experimental data [28] correspond to 9.32 and 8.93 for such inclusion compounds, respectively. The experimental trend was not achieved even with the additional scan for the (+) camphor guest associated with the α-CD. If the four 1:2 systems were considered, an $R^2 = 0.6575$ is obtained at this stage. Through the linear correlation, with $\log \beta_{12} = 1.0904(xTB) + 1.6529$, the errors for estimated log β_{12} predicted vary from 5 to 16%. The issue is related to the underestimated log β_{12} computed at GNF2-xTB (ALPB) level of theory for the (+) camphor@(α-CD)$_2$. If the log β_{12} data for (+) camphor@(α-CD)$_2$ is excluded, a linear correlation with $R^2 = 0.9902$ is obtained. The errors computed with data for (+) fenchone@(α-CD)$_2$, (−) fenchone@(α-CD)$_2$, and (−) camphor@(α-CD)$_2$ vary from 1 to 3% what is coherent to our

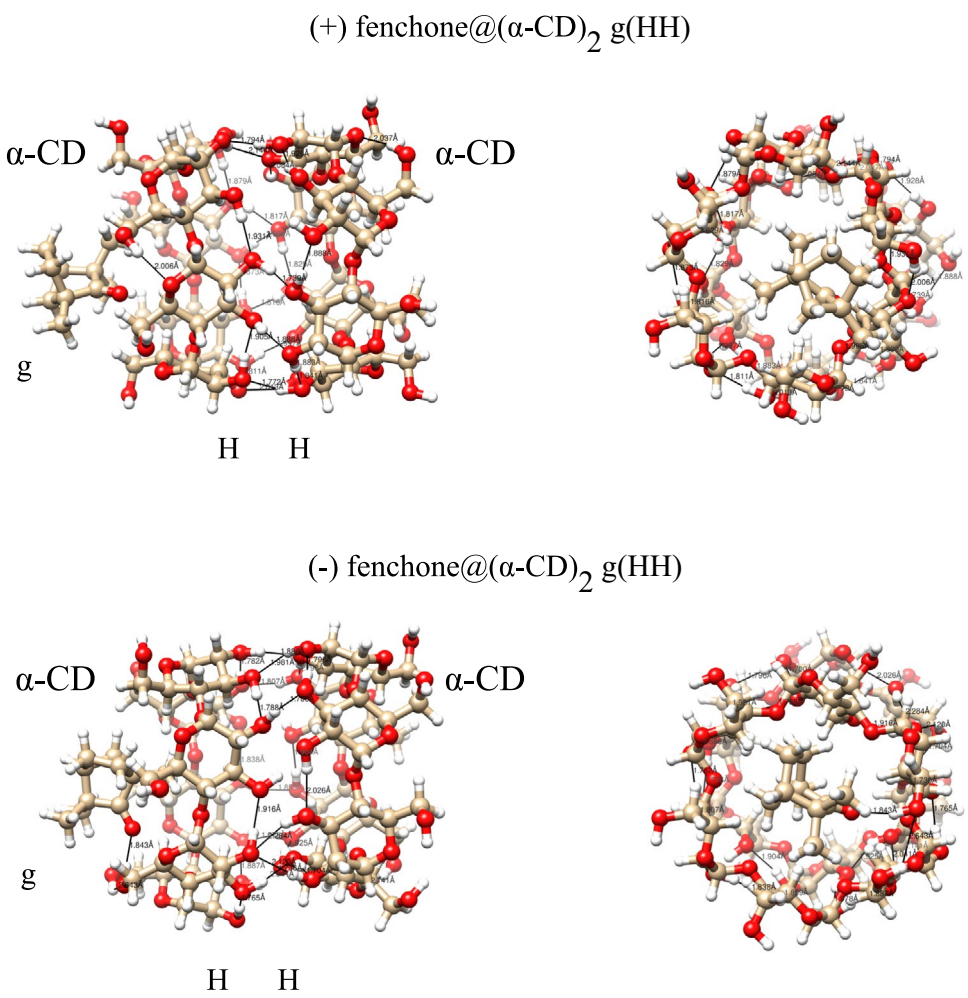

Fig. 4 Spatial arrangements of the most stable fenchone@$(CD)_2$ systems optimized at GFN2-xTB (ALPB) level of theory (C-A and A-A for (+) and (−) fenchone, respectively associated with two CDs, in Table 2). The identification of the guest spatial orientation concerning the CD cavity (gHH) is also indicated. Many intermolecular hydrogen bonds between the CD units are shown

previous study [23]. Therefore, as previously discussed, some representative (+) camphor@$(\alpha\text{-CD})_2$ were not identified. Such information serves as a guide to improve the exploration of the GFN2-xTB level of theory.

Table 2 shows three types of $(\alpha\text{-CD})_2$ associations identified by the capital letters A-, D-, and E-. Those arrangements correspond to HgH associations. The UD-APARM software was then modified to account for symmetry molecules and to allow the study of arrangements with the $(\alpha\text{-CD})_2$ system as the reference. The modification was necessary because the UD-APARM original implementation deals with the center of mass of a set of atoms (oxygen for CDs) to determine the positive directions of the Cartesian axes mounted over the axes of inertia of the reference system (or molecule). A CD association such as HH comprises a center of mass of oxygen atoms (due to symmetry) very close to the center of mass of the entire system. After the modifications in the UD-APARM code, it became possible to keep $(\alpha\text{-CD})_2$ structures obtained from D-A, E-A, and A-A (Table 2) and rotate the (+) camphor guest inside the $(\alpha\text{-CD})_2$ according to the parameters listed in Table S4. The parameters implied in an additional 853 new (+) camphor@$(\alpha\text{-CD})_2$ (HgH) for each scan, totaling additional 2559 (3×853) starting inclusion compounds to be optimized at GFN2-xTB level of theory.

Within a 3.0 kcal mol^{-1} window, the data for the new (+) camphor@$(\alpha\text{-CD})_2$ (HgH) obtained from such a study were included in Table 3. From (+) camphor@$(\alpha\text{-CD})_2$ (HgH) originated from A-A, D-A, and E-A, the most stable Gibbs energies in solution correspond to − 7.86, − 10.16, and − 7.40 kcal mol^{-1}, respectively. From Table 3, we see twenty (+) camphor@$(\alpha\text{-CD})_2$ obtained with the D-A HH association (D-A-1 to D-A-20), three for A-A (A-A-1 to A-A-3) and two for E-A (E-A-1 and E-A-2). All contribute to the log β_{12} that, at this stage, corresponds to 7.75. The value of log β_{12} for (+) camphor@$(\alpha\text{-CD})_2$ is greater than that of (−) camphor@$(\alpha\text{-CD})_2$ (see Table 2).

An interesting aspect in Table 3 corresponds to the variation in the association parameters, such as α and β-Euler angles. Such variation implies multiple guest positions inside the capsule formed by the two α-CD units in a head-to-head (HH) arrangement. The optimized structures of the D-A associations from 1 to 14 that comprise 93.2% of the binding constant for the (+) camphor@$(\alpha\text{-CD})_2$ are shown in Fig. 6. The analysis of the oxygen atoms of the guest

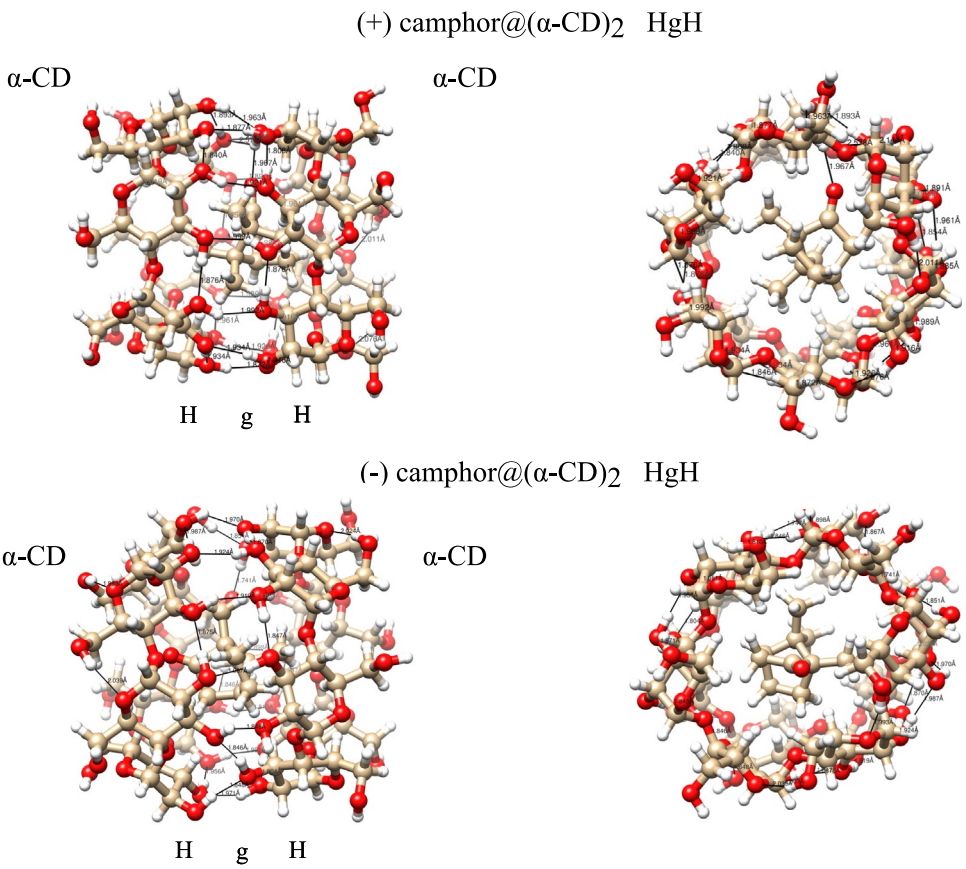

Fig. 5 Spatial arrangements of the most stable camphor@$(\alpha\text{-CD})_2$ systems optimized at GFN2-xTB (ALPB) level of theory (D-A and B-A for (+) and (−) camphor, respectively associated with two CDs, in Table 2). The identification of the guest spatial orientation concerning the CD cavity (HgH) is also indicated. Many intermolecular hydrogen bonds between the CD units are shown

(see Fig. 6) indicates that multiple positions can be found at equilibrium for (+) camphor@$(\alpha\text{-CD})_2$. Such multiple positions in solution predicted by GFN2-xTB (ALPB) level of theory are expected to be found in the solid state. The overall arrangements depicted in Fig. 6 (and also in Fig. 5) are coherent to crystal structures for which dimeric molecules of α-CD bonded in a head-to-head (HH) arrangement contain camphor guest species in the cavity formed by the two CD molecules [39, 40]. Furthermore, the experimental findings support GFN2-xTB (ALPB) theory-predicted multiple positions (Table 3; Fig. 6) for the inclusion of (+) camphor into α-CD. According to a recent X-ray study, the crystal data addressed the orientational disordering of (+) camphor molecules inside the cavity formed by two α-CD bonded in an HH arrangement [40].

Concerning the binding constants, the experimental trend was achieved with an excellent linear correlation. The data of the present study at the GFN2-xTB (ALPB) level of theory, obtained using the UD-APARM as a tool to explore the PES, are shown in Table 4. In the first line of Table 4, we see that four inclusion compounds were used for (+) fenchone to obtain the log K_1 and eight to obtain the log β_{12}. We see from Table 4 that a higher number of systems for 1:2 inclusion compounds is used to obtain the theoretical values than 1:1, except for (−) camphor included in α-CD (with only one system to 1:2 system). The GFN2-xTB (ALPB) data for log K_1 for camphor@α-CD (1.42 and 2.02) are higher than estimated for fenchone@α-CD (0.90 and 0.23), being the latter coherent to the experimental trend [28]. For the GFN2-xTB (ALPB) data concerning log β_{12}, we see that camphor@$(\alpha\text{-CD})_2$ values (7.18 and 7.75) are higher than estimated for fenchone@$(\alpha\text{-CD})_2$ (4.10 and 5.06) what is coherent to the experimental trend. For camphor and fenchone, we see that the (+) isomer interacting with $(\alpha\text{-CD})_2$ presented an overall binding constant higher than the (−) isomer. This trend is coherent with experimental findings.

According to Table 4, at the GFN2-xTB (ALPB) level of theory, chiral recognition was achieved for the four inclusion compounds investigated: (+)-fenchone@$(\alpha\text{-CD})_2$, (−)-fenchone@$(\alpha\text{-CD})_2$, and (−)-camphor@$(\alpha\text{-CD})_2$ and (+)-camphor@$(\alpha\text{-CD})_2$. A good linear correlation between experimental and theoretical log β_{12} with an R^2 equal to 0.9933 was computed. When experimental and theoretical adjusted GFN2-xTB (ALPB) binding constants were compared, the estimated error varied from 1 to 3%. The linear correlation between experimental and theoretical log β_{12} is shown in Fig. 7.

The most stable guest@$(\alpha\text{-CD})_2$ systems obtained at the GFN2-xTB (ALPB) were investigated through DFT at the B97-D/6-31G(d,p) level of theory. The DFT method was

Table 3 Association free energies (ΔG_{water}) in continuum ALPB model, and the corresponding supramolecular main parameters (APARM data) for relative position (r, θ) and relative rotation (α, β, and γ) for representative camphor@(α-CD)$_2$ systems obtained after modification of the rotation and position the guest inside the A-A, D-A, and E-A (α-CD)$_2$ associations

Compound	log β_{12}	ID	Spatial representation	ΔG_{water} (kcal mol^{-1})	r (Å)	θ (deg)	α (deg)	β (deg)	γ (deg)
(+)camphor@(α-CD)$_2$	7.75	D-A 1	HgH	− 10.16	0.6	87	191	68	44
		D-A 2	HgH	− 9.32	0.5	63	33	279	38
		D-A 3	HgH	− 9.15	0.4	85	301	277	57
		D-A 4	HgH	− 9.11	0.6	115	110	216	326
		D-A 5	HgH	− 8.99	0.5	112	195	234	332
		D-A 6	HgH	− 8.49	0.4	94	312	110	335
		D-A 7	HgH	− 8.46	0.6	95	332	304	70
		D-A 8	HgH	− 8.43	0.4	158	298	168	335
		D-A 9	HgH	− 8.39	0.2	18	106	81	57
		D-A 10	HgH	− 8.34	0.5	109	143	102	354
		D-A 11	HgH	− 8.24	0.5	105	168	234	84
		D-A 12	HgH	− 8.09	0.7	73	235	79	40
		D-A− 13	HgH	− 8.00	0.5	110	85	81	281
		D-A-14	HgH	− 8.00	0.6	118	222	270	285
		A-A-1	HgH	− 7.86	0.5	129	259	151	33
		D-A-15	HgH	− 7.83	0.4	19	109	348	348
		A-A-2	HgH	− 7.80	0.4	132	263	153	34
		A-A-3	HgH	− 7.77	0.4	37	272	335	63
		D-A-16	HgH	− 7.67	0.5	96	19	107	333
		D-A-17	HgH	− 7.55	0.3	76	89	239	49
		D-A-18	HgH	− 7.52	0.3	69	305	274	316
		D-A-19	HgH	− 7.47	0.4	44	283	341	355
		E-A-1	HgH	− 7.40	0.5	82	207	92	51
		E-A-2	HgH	− 7.32	0.5	80	213	97	53
		D-A-20	HgH	− 7.25	0.3	124	36	195	284

The GFN2-xTB (ALPB) log β_{12} was computed in a multi-equilibrium approach at 300.6 K from the optimization of 2559 systems

Table 4 Theoretical (GFN2-xTB) and experimental [28, 29] association constants (log K_1 and log β_{12}) for 1:1 and 1:2 inclusion compounds formed with camphor, fenchone enantiomers, and α-CD at 300.6 K

host	Distinct systems 1:1	GFN2-xTB log K_1	Expt. log K_1	Distinct systems 1:2	GFN2-xTB log β_{12}	Expt. log β_{12}	Adjusted[a] GFN2-xTB log β_{12}	Error[b] %
(−) fenchone	1	0.23	2.72	3	4.10	5.83	5.72	2
(+) fenchone	4	0.90	2.74	8	5.06	6.51	6.68	3
(−) camphor	8	2.02		1	7.18	8.93	8.81	1
(+) camphor	5	1.42		25	7.75	9.32	9.38	1

18,615 starting systems (8,640 for 1:1 guest/CD and 5,184 + 2,232 + 2,559 for 1:2 guest/CD stoichiometry) were obtained with UD-APARM and investigated as GFN2-xTB (ALPB) level of theory

[a] $y = 1.0018x + 1.6141$, $R^2 = 0.9936$

[b] Error = 100 × [Adusted GFN2-xTB log β_{12} – Expt. log β_{12})/Expt. Log]

chosen based on our previous contribution [41] related to the CD-based host-guest systems. The four most stable arrangements (from Tables 2 and 3) were optimized using the vacuum and the SMD continuum model implemented in the ORCA package. The analysis was not exhaustive. Due to the computational cost associated with the systems under investigation, the GFN2-xTB thermal correction to Gibbs energy was considered. The original data for GFN2-xTB (ALPB) and the new B97-D/6-31G(d,p) were included in Tables S5 and S6 (Supplementary Information file). At the B97-D/6-31G(d,p), the camphor@(α-CD)$_2$ systems are more stable than the fenchone@(α-CD)$_2$ systems. However, from

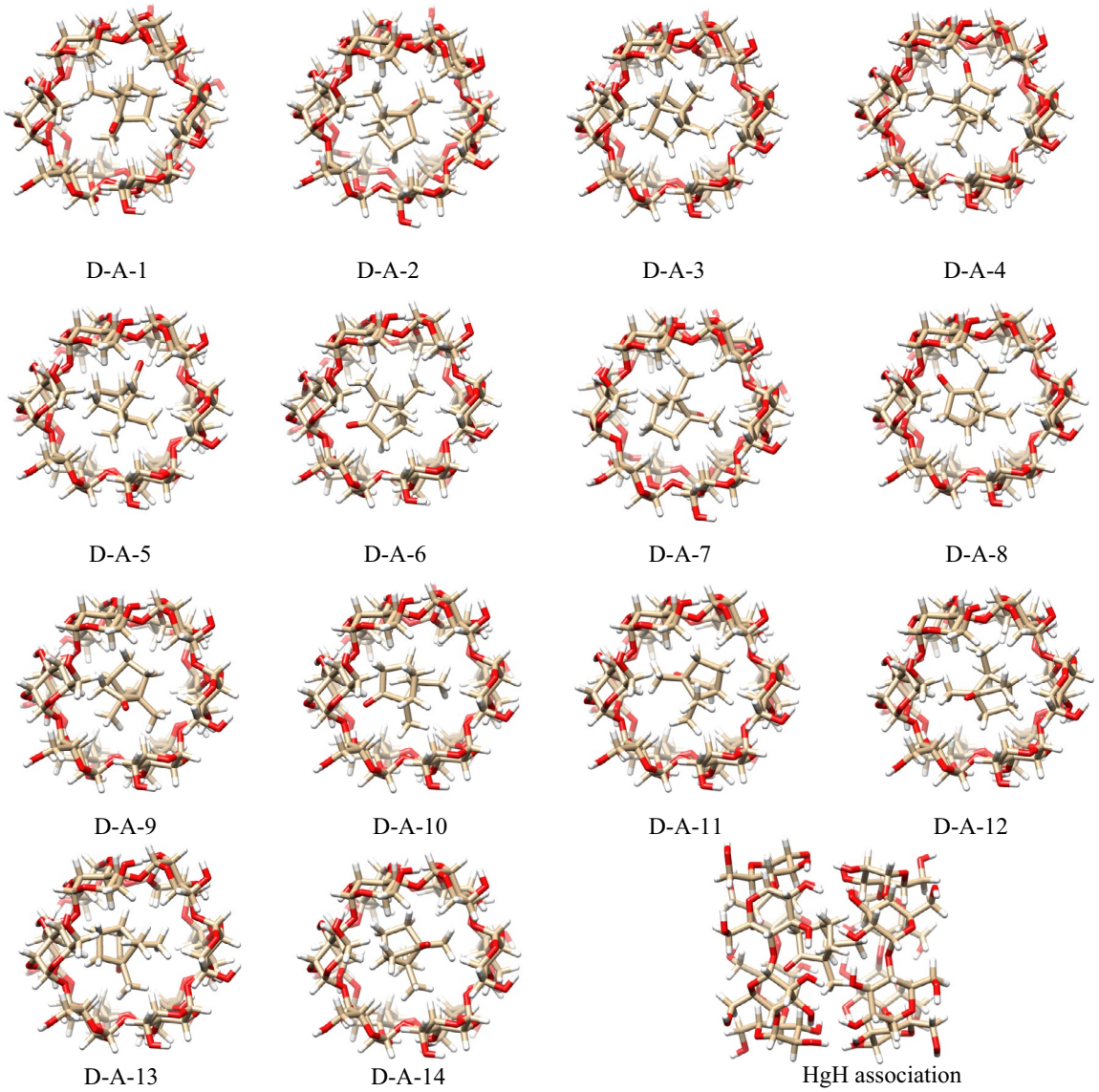

Fig. 6 Spatial arrangements of the most stable (+) camphor@$(\alpha\text{-CD})_2$ systems optimized at GFN2-xTB (ALPB) level of theory (D-A-1 to D-A-14, see Table 3) comprising 92.3% of the theoretical binding constant. We see multiple guest orientation inside the HH arrangement formed by two CD units as addressed experimentally for solid state [40]

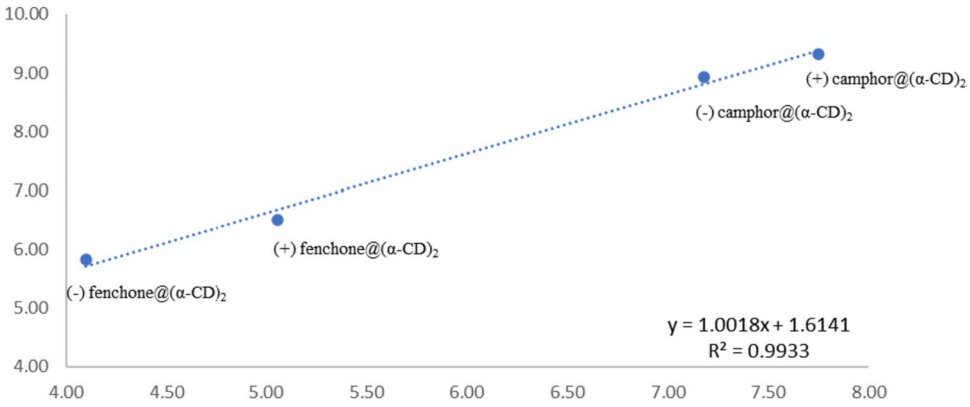

Fig. 7 Linear correlation obtained between experimental and GFN2-xTB (ALPB) log β_{12} with data for all guest@$(CD)_2$ (left) and with the exclusion of the data for (+) camphor@$(\alpha\text{-CD})_2$ system (right)

the analysis of Table S6, the experimental trend was not achieved. The geometries obtained at GFN2-xTB and B97-D/6-31G(d,p) are very close (see the superpositions shown in Fig. S1). From the data (Tables S5 and S6), it can be stated that the local minimum does not coincide when GFN2-xTB and B97-D/6-31G(d,p) levels of theory are compared. Data in Tables S5 and S6 suggest that the PES exploration should be carried out at the B97-D level of theory, which is prohibitive in terms of computational cost. To address a definitive conclusion concerning the comparison between B97-D and GFN2-xTB outcomes, a new investigation that is beyond the scope of the present contribution must be carried out.

The CREST software was employed in the final analysis of the present contribution because such software can be used to investigate non-bonded systems. Initially, before obtaining the data in Table 2, the most stable camphor@$(\alpha\text{-CD})_2$ systems, D-A for (+) camphor and B-A for (−) camphor included in $(\alpha\text{-CD})_2$ (see Table 3), were used as the starting geometries to perform the CREST's NCI mode evaluation. The geometries obtained by CREST were submitted to the GFN2-xTB optimization using ALPB, as carried out previously with UD-APARM geometries, for comparison. The first analysis of Table S7 attests that CREST gives rise to more stable systems than those obtained with the GFN2-xTB (ALPB) /UD-APARM approach adopted herein. The computational cost associated with such investigation is very high (see Fig. S2). What is curious is that after obtaining the data in Table 3, the most stable arrangement identified for (+) camphor@$(\alpha\text{-CD})_2$ D-A-1, submitted as the starting geometry for CREST NCI, gives a distinct non-bonded arrangement, most stable than (−) camphor@$(\alpha\text{-CD})_2$ following the experimental trend (see Table S7). According to Table S7, the CREST outcome (crest_best.xyz) depends on the starting geometry. We see from Table S7 that the data obtained from D-A (Table 2) and D-A-1 (Table 3) starting geometries are very distinct. The study discussed here should be conducted from 1:1 and 1:2 guest/host systems with other structures beyond the crest_best.xyz file (obtained with CREST) to account for the multi-equilibrium approach and remove the influence of the UD-APARM/GNF2-xTB search to address the application of the CREST software to the present discussion. The potential use of CREST to study complex CD-based host-guest systems is under study in my research group. Still, the reproduction of the present work without the influence of the UD-APARM software is beyond the scope of the present work. Finally, caution is required in the use of CREST for CDs. According to a previous investigation (data not shown), the best structure obtained for an isolated CD (crest_best.xyz) corresponds to a system with an almost close cavity (that precludes inclusion for one rim) similar to the structure 1(+) reported previously for the quantum conformational study of α-CD [42]. Such a CD structure is not representative (in aqueous media). Finally, it is worth noting that CREST was used successfully to obtain the guest starting geometries (not the host's geometries) in our recent contributions [22, 23], and its use is still under investigation. However, the present test for CREST was carried out with systems obtained by the UD-APARM/GFN2-xTB approach; therefore, the isolated contribution of such software cannot be addressed.

At this point, a brief discussion concerning other CD-based chiral recognition theoretical approaches shed light on the applicability of the GFN2-xTB (ALPB) multi-equilibrium methodology. With Molecular Mechanics (MM), Lipkowitz et al. [43] studied the enantiodifferentiation in solid-state cyclodextrin through the use of MM2 [44] and AMBER [45] force fields as implemented in Macromodel [46]. Among the systems investigated, selectivity for (RS)-fenoprofen by β-CD is supported by the only experimental data used as a reference [47]. Lipkowitz et al. determined theoretically that the S-enantiomer of fenoprofen is more tightly bound to the β-CD host. In another contribution, Lipkowitz and Stoehr investigated the enantiodifferentiation of (RS)-methyl mandelate through β-CD in the liquid phase in detail [48]. Molecular mechanics and MD were critically discussed by Dodziuk et al. in subsequent contributions [48]. Despite the discussion concerning Classical Mechanics, MD was successfully used to study chiral discrimination of (RS)-ibuprofen isomers included in β-CD [49]. Within such a contribution of Núñez-Agüero et al., the ΔΔG evaluated with the MM-PBSA/GBSA method [50] applied after an MD production agrees with the experiment for which S-ibuprofen is more stable than R-ibuprofen. Through the use of quantum methods, an interesting contribution of Yan et al. concerning the (+)-catechin and (−)-epicatechin included in β-CD was carried out with the optimization of many starting systems at a distinct distance with PM3 [51] level of theory [52]. Within Yan et al. contribution [52], single-point calculations were carried out with B3LYP (Becke three-parameter, Lee-Yang-Parr exchange) [53, 54] and Hartree-Fock (HF) [55] formalisms with 6-31G* basis set. The authors concluded that (+)-catechin forms the most stable complex with β-CD. An interesting contribution from a joint experimental-theoretical was conducted by Reyes-Reyes et al. concerning the chiral recognition of abacavir (ABA) enantiomers by (2-hydroxy) propyl-β-CD (2HPβCD) [56]. Within such a study, the Density Functional Theory (DFT) at PBE/6–31 G** level of theory [57] with the Polarizable Continuum Model (PCM) [58] to account for the solvent effect were used. The theoretical interaction energies computed for the inclusion of ABA into 2HPβCD corroborate the experimental trend addressed by the apparent stability constants. The combination of Molecular Docking, semiempirical, and DFT was also applied within CD-based systems to chiral recognition. For instance, we have Arsad et al. contribution concerning the discrimination of ketoconazole enantiomers

through modified β-CD (TMβ-CD) [59]. The theoretical data correlated to their previous experimental work [60] in which the separation of four ketoconazole stereoisomers was successfully carried out using Electrokinetic Chromatography (EKC) with TMβ-CD as a chiral selector. Within more recent contributions, we see the combination of more than one classical method, such as Docking followed by MD and Docking followed by the use of the ONIOM [61] approach with PM6 [61] and B3LYP/6-31G++(d,p) for low and high layers, respectively, as carried out in the study of (R/S)-noradrenaline included in β-CD [62]. Within such a contribution, the high stability of the S-noradrenaline included in β-CD obtained theoretically based on ΔG corroborates with experimental information [62].

The approach discussed herein developed with the use of UD-APARM, GFN2-xTB, the continuum solvent ALPB in a multi-equilibrium approach differs from the discussed theoretical applications to CD-based chiral recognition mainly due to the possibility of estimating binding constants. A trend or a rank is also obtained by the approach adopted in the present study. The binding constant evaluation consists of a step forward in the predictive capacity of theoretical methodologies. The limitation of the GFN2-xTB (ALPB) multi-equilibrium approach relies on adjusting at least three experimental binding data to predict unknown data for homologous guests included in a studied CD. Evaluating a theoretical trend without any dependency on experimental information depends on a massive exploration of the PES of the theoretical method employed to compute the binding constants and a task also focused on in my research group.

Conclusion

Within the present work, chiral recognition of camphor and fenchone enantiomers by α-CD was investigated theoretically at the GFN2-xTB (ALPB) level of theory in a multi-equilibrium scope with the use of the UD-APARM software. For 1:1 associations, from the investigation of 8,640 supramolecular associations, only 37 (0.43%) were identified, with $\Delta G_{water} < 0$ being 18 (0.21%) distinct or non-equivalent supramolecular systems. For 1:2 associations, 45 (0.45%) contribute to the binding constants. After the GFN2-xTB (ALPB) study of 18,615 starting systems obtained through the UD-APARM software, the chiral recognition was achieved for the four inclusion compounds investigated: (−)-fenchone@$(\alpha\text{-CD})_2$, (+)-fenchone@$(\alpha\text{-CD})_2$, and (−)-camphor@$(\alpha\text{-CD})_2$ and (+)-camphor@$(\alpha\text{-CD})_2$. When experimental and theoretical GFN2-xTB (ALPB) binding constants were compared, a linear correlation with an R^2 equal to 0.9933 was obtained. Estimated error varied from 1 to 3% to adjusted GFN2-xTB values. B97-D/6-31G(d,p) and CREST calculations were carried out, but a definitive conclusion concerning their application to the systems under investigation cannot be addressed. The use of CREST to treat CD-based host-guest systems is under investigation.

Supplementary Information The online version contains supplementary material available at https://doi.org/10.1007/s10847-024-01219-3.

Acknowledgements The author thanks Professor Hélio Ferreira dos Santos for the access to the NEQC (Núcleo de Estudos em Química Computacional, UFJF, Brazil) computer facility and also thanks the Laboratório Central de Computação Científica (LCC) da UFLA for providing additional computing resources. Furthermore, also thanks to the Fundação de Amparo à Pesquisa do Estado de Minas Gerais (FAPEMIG) for supporting the Laboratório de Química Fundamental (LQF), where the research was conducted.

Author contributions CPAA proposed the research, obtained the data, and wrote and revised the manuscript.

Declarations

Competing interest The author declares no competing interest.

References

1. Szejtli, J.: Introduction and general overview of cyclodextrin chemistry. Chem. Rev. **98**(5), 1743–1753 (1998). https://doi.org/10.1021/cr970022c
2. Crini, G., Review: A history of cyclodextrins. Chem. Rev. **114**(21), 10940–10975 (2014). https://doi.org/10.1021/cr500081p
3. Del Valle, E.M.M.: Cyclodextrins and their uses: a review. Process. Biochem. **39**(9), 1033–1046 (2004). https://doi.org/10.1016/S0032-9592(03)00258-9
4. Matencio, A., Navarro-Orcajada, S., García-Carmona, F., López-Nicolás, J.M.: Applications of cyclodextrins in food science. A review. Trends Food Sci. Technol. **104**, 132–143 (2020). https://doi.org/10.1016/j.tifs.2020.08.009
5. Loftsson, T., Duchêne, D.: Cyclodextrins and their pharmaceutical applications. Int. J. Pharm. **329**, 1–2 (2007). https://doi.org/10.1016/j.ijpharm.2006.10.044
6. Landy, D., Mallard, I., Ponchel, A., Monflier, E., Fourmentin, S.: Remediation technologies using cyclodextrins: an overview. Environ. Chem. Lett. **10**(3), 225–237 (2012). https://doi.org/10.1007/s10311-011-0351-1
7. Yadav, M., Thakore, S., Jadeja, R.: A review on remediation technologies using functionalized cyclodextrin. Environ. Sci. Pollut Res. **29**(1), 236–250 (2022). https://doi.org/10.1007/s11356-021-15887-y
8. Waris, K.H., Lee, V.S., Mohamad, S.: Pesticide remediation with cyclodextrins: a review. Environ. Sci. Pollut Res. **28**, 47785–47799 (2021). https://doi.org/10.1007/s11356-021-15434-9
9. Sikder, M.T., Rahman, M.M., Jakariya, M., Hosokawa, T., Kurasaki, M., Saito, T.: Remediation of water pollution with native cyclodextrins and modified cyclodextrins: a comparative overview and perspectives. Chem. Eng. J. **355**, 920–941 (2018). https://doi.org/10.1016/j.cej.2018.08.218
10. Scriba, G.K.E.: Chiral recognition in separation science–an update. J. Chromatogr. A **1467**, 56–78 (2016). https://doi.org/10.1016/j.chroma.2016.05.061
11. Wang, Y., Zhuo, S., Hou, J., Li, W., Ji, Y.: Construction of β-cyclodextrin covalent organic framework-modified chiral

stationary phase for chiral separation. ACS Appl. Sci. Interfaces (2019). https://doi.org/10.1021/acsami.9b16720
12. Easton, C.J., Lincoln, S.F.: Chiral discrimination by modified cyclodextrins. Chem. Soc. Rev. **25**, 163–170 (1996)
13. Rekharsky, M., Inoue, Y.: Chiral recognition thermodynamics of -cyclodextrin: the thermodynamic origin of enantioselectivity and the enthalpy–entropy compensation effect. J. Am. Chem. Soc. **33**, 4418–4435 (2023)
14. Armstrong, D.W., Ward, T.J., Armstrong, R.D., Beesley, T.E.: Separation of drug stereoisomers by the formation of β-cyclodextrin inclusion complexes. Science **232**, 1132–1135 (1986)
15. Rekharsky, M., Inoue, Y.: Chiral recognition thermodynamics of β-Cyclodextrin: The thermodynamic origin of Enantioselectivity and the Enthalpy - Entropy Compensation Effect. J. Am. Chem. Soc. **122**(33), 4418–4435 (2000)
16. Casadesús, R., Moreno, M., González-Lafont, À., Lluch, J.M., Repasky, M.P.: Testing electronic structure methods for describing intermolecular H...H interactions in supramolecular chemistry. J. Comput. Chem. **25**(1), 99–105 (2004)
17. Bannwarth, C., Ehlert, S., Grimme, S.: GFN2-xTB-an accurate and broadly parametrized self-consistent tight-binding quantum chemical method with multipole electrostatics and density-dependent dispersion contributions. J. Chem. Theory Comput. **15**(3), 1652–1671 (2019). https://doi.org/10.1021/acs.jctc.8b01176
18. Grimme, S., Bannwarth, C., Shushkov, P., Robust, A.: Accurate tight-binding quantum chemical method for structures, vibrational frequencies, and noncovalent interactions of large molecular systems parametrized for all spd-block elements (Z = 1–86). J. Chem. Theor. Comput. **13**(5), 1989–2009 (2017). https://doi.org/10.1021/acs.jctc.7b00118
19. Usacheva, T.R., et al.: Complexation of cyclodextrins with benzoic acid in water-organic solvents: a solvation-thermodynamic approach. Molecules (2021). https://doi.org/10.3390/molecules26154408
20. Ferrero, R., et al.: On the interactions of melatonin/β-cyclodextrin inclusion complex: a novel approach combining efficient semiempirical extended tight-binding (xTB) results with ab Initio methods. Molecules **26**(19), 5881 (2021). https://doi.org/10.3390/molecules26195881
21. Anconi, C.P.A.: Relative position and relative rotation in supramolecular systems through the analysis of the principal axes of Inertia: ferrocene/cucurbit[7]uril and ferrocenyl azide/β-cyclodextrin case studies. ACS Omega **5**(10), 5013–5025 (2020). https://doi.org/10.1021/acsomega.9b03914
22. Anconi, C.P.A., Souza, L.C.A.: Multi-equilibrium approach to study cyclodextrins host–guest systems with GFN2-xTB quantum method: A case study of phosphorothioates included in β-cyclodextrin. Comput. Theor. Chem. **1217**, 113916 (2022)
23. Campos, J., Carolina, M., Cardoso, L., Gleicy, R., Erick, T., Lacerda, F.: Inclusion of paraoxon, parathion, and methyl parathion into α–cyclodextrin: A GFN2–xTB multi–equilibrium quantum study. J. Incl. Phenom. Macrocycl. Chem. **103**, 263–276 (2023). https://doi.org/10.1007/s10847-023-01192-3
24. Kim, S., et al.: PubChem in 2021: new data content and improved web interfaces. Nucleic Acids Res. (2021). https://doi.org/10.1093/nar/gkaa971
25. Puliti, R., Mattia, C.A., Paduano, L.: Crystal structure of a new α-cyclodextrin hydrate form molecular geometry and packing features: disordered solvent contribution. Carbohydr. Res. **310**, 1–2 (1998). https://doi.org/10.1016/S0008-6215(98)00150-5
26. Bannwarth, C., et al.: Extended tight-binding quantum chemistry methods. Wiley Interdiscip. Rev. Comput. Mol. Sci. **11**, 1–49 (2021). https://doi.org/10.1002/wcms.1493
27. Ehlert, S., Stahn, M., Spicher, S., Grimme, S.: Robust and efficient implicit solvation model for fast semiempirical methods. J. Chem. Theor. Comput. **17**(7), 4250–4261 (2021). https://doi.org/10.1021/acs.jctc.1c00471
28. Nowakowski, M., Ejchart, A.: Complex formation of fenchone with α-cyclodextrin: NMR titrations. J. Incl. Phenom. Macrocycl. Chem. **79**, 337–342 (2014). https://doi.org/10.1007/s10847-013-0356-4
29. Bernatowicz, P., Nowakowski, M., Dodziuk, H., Ejchart, A.: Determination of association constants at moderately fast chemical exchange: complexation of camphor enantiomers by a -cyclodextrin. J. Magn. Reson. **181**, 304–309 (2006). https://doi.org/10.1016/j.jmr.2006.06.001
30. Grimme, S.: Semiempirical GGA-type density functional constructed with a long-range dispersion correction. J. Comput. Chem. **27**, 1787–1799 (2006). https://doi.org/10.1002/jcc.20495
31. Marenich, A.V., Cramer, C.J., Truhlar, D.G.: Universal solvation model based on solute electron density and on a continuum model of the solvent defined by the bulk dielectric constant and atomic surface tensions. J. Phys. Chem. B. **113**(18), 6378–6396 (2009)
32. Neese, F.: The ORCA program system. Wiley Interdiscip. Rev. Comput. Mol. Sci. **2**(1), 73–78 (2012)
33. Pracht, P., Bohle, F., Grimme, S.: Automated exploration of the low-energy chemical space with fast quantum chemical methods. Phys. Chem. Chem. Phys. **22**, 7169–7192 (2020). https://doi.org/10.1039/c9cp06869d
34. Anconi, C.P.A., Nascimento, C.S., De Almeida, W.B., Dos Santos, H.F.: The role played by head-tail configuration on the molecular weight distribution of α-cyclodextrin tubes. J. Incl. Phenom. Macrocycl. Chem. **60**, 1–2 (2008). https://doi.org/10.1007/s10847-007-9348-6
35. Bonnet, P., Jaime, C., Morin-allory, L.: Structure and thermodynamics of α-, β-, and γ-cyclodextrin dimers. molecular dynamics studies of the solvent effect and free binding energies. J. Org. Chem. **19**, 8602–8609 (2002)
36. Dodziuk, H., Nowinski, K.S., Dolgonos, G.: On the impossibility of determination of stepwise binding constants for the 1: 2 complex of (+)-camphor with α-cyclodextrin. Org. Biomol. Chem. no. **1**, 581–584 (2003)
37. Dodziuk, H., Ejchart, A., Lukin, O., Vysotsky, M.O.: 1H and 13 C NMR and molecular dynamics study of chiral recognition of camphor enantiomers by α-cyclodextrin. J. Org. Chem. no. **64**(5), 1503–1507 (1999)
38. Lopes, J.F., Nascimento, C.S., Anconi, C.P.A., Santos, H.F.D., Almeida, W.B.D.: Inclusion complex thermodynamics: The β-cyclodextrin and sertraline complex example. J. Mol. Graph Model. **62**, 11–17 (2015). https://doi.org/10.1016/j.jmgm.2015.08.008
39. Kokkinou, A., Tsorteki, F., Karpusas, M., Papakyriakou, A., Bethanis, K.: Study of the inclusion of the (R)- and (S)-camphor enantiomers in α-cyclodextrin by X-ray crystallography and molecular dynamics. Carbohydr. Res. no. **345**(8), 1034–1040 (2010). https://doi.org/10.1016/j.carres.2010.03.020
40. Lipkowski, J., Bielejewska, A., Presly, O.: Pseudo-polymorphism of a camphor α-cyclodextrin complex. Carbohydr. Res. no. **520**, 108601 (2022). https://doi.org/10.1016/j.carres.2022.108601
41. Pereira, R.A., da Silva Borges, W.M., Peraro, C.R., Anconi, C.P.A.: Theoretical inclusion of deprotonated 2,4-D and dicamba pesticides in ß-cyclodextrin. J. Incl. Phenom. Macrocycl. Chem. no. **86**, 3–4 (2016). https://doi.org/10.1007/s10847-016-0665-5
42. Anconi, C.P.A., Nascimento, C.S., Fedoce-Lopes, J., Dos Santos, H.F., De Almeida, W.B.: Ab initio calculations on low-energy conformers of α-cyclodextrin. J. Phys. Chem. A. no. **111**(48), 12127–12135 (2007). https://doi.org/10.1021/jp0762424

43. Lipkowitz, K.B., Green, K.M., Yang, J., Pearl, G., Peterson, M.A.: Theoretical study of enantiodifferentiation in solid state cyclodextrins. Chirality **5**, 51–57 (1993)
44. Allinger, N.L.: Conformational analysis. 130. MM2. A hydrocarbon force field utilizing V1 and V2 torsional terms. J. Am. Chem. Soc. **99**(25), 8127–8134 (1977). (**.**)
45. Weiner, P.K., Kollman, P.A.: AMBER: assisted model building with energy refinement. a general program for modeling molecules and their interactions. J. Comput. Chem. **2**(3), 287–303 (1981)
46. Mohamadi, F., et al.: Macromodel—an integrated software system for modeling organic and bioorganic molecules using molecular mechanics. J. Comput. Chem. no. **11**(4), 440–467 (1990)
47. Hamilton, J.A., Chen, L.: Crystal structure of an inclusion complex of β-cyclodextrin with racemic fenoprofen: direct evidence for chiral recognition. J. Am. Chem. Soc. **110**(17), 5833–5841 (1988)
48. Lipkowitz, K.B., Stoehr, C.M.: Detailed experimental and theoretical analysis of chiral discrimination: enantioselective binding of R/S methyl mandelate by β-cyclodextrin. Chirality **8**, 341–350 (1996)
49. Núñez-Agüero, C.-J., Escobar-Llanos, C.-M., Díaz, D., Jaime, C., Garduño-Juárez, R.: Chiral discrimination of ibuprofen isomers in β-cyclodextrin inclusion complexes: experimental (NMR) and theoretical (MD, MM/GBSA) studies. Tetrahedron **62**, 4162–4172 (2006). https://doi.org/10.1016/j.tet.2006.02.010
50. Srinivasan, J., Cheatham, T.E., Cieplak, P., Kollman, P.A., Case, D.A.: Continuum solvent studies of the stability of DNA, RNA, and phosphoramidate-DNA helices. J. Am. Chem. Soc. **120**(37), 9401–9409 (1998)
51. Stewart, J.J.P.: Optimization of parameters for semiempirical methods II. Applications. J. Comput. Chem. no. **10**(2), 221–264 (1989)
52. Yan, C., Xiu, Z., Li, X., Hao, C.: Molecular modeling study of β-cyclodextrin complexes with (+) -catechin and (−)-epicatechin. J. Mol. Graph Model. **26**, 420–428 (2007). https://doi.org/10.1016/j.jmgm.2007.01.010
53. Becke, A.D.: Density-functional thermochemistry. III. The role of exact exchange. J. Chem. Phys. no. **98**, 5648–5652 (1993)
54. Lee, C., Yang, W., Parr, R.H.: Into a functional of the electron density f f. Phys. Rev. B. no. **37**(2), 785–789 (1988)
55. Laaksonen, L., Pyykkö, P., Sundholm, D.: Fully numerical Hartree-Fock methods for molecules. Comput. Phys. Rep. **4**(5), 313–344 (1986)
56. Reyes-Reyes, M.L., et al.: Chiral recognition of abacavir enantiomers by (2-hydroxy) propyl-β-cyclodextrin: UHPLC, NMR and DFT studies. J. Incl. Phenom. Macrocycl. Chem. no. **82**, 373–382 (2015). https://doi.org/10.1007/s10847-015-0499-6
57. Adamo, C., Barone, V.: Toward reliable density functional methods without adjustable parameters: the PBE0 model. J. Chem. Phys. **110**, 6158–6170 (1999)
58. Scalmani, G., Frisch, M.J.: Continuous surface charge polarizable continuum models of solvation. I. General formalism. J. Chem. Phys. no. **132**, 114110 (2010). https://doi.org/10.1063/1.3359469
59. Arsad, S.R., Maarof, H., Ibrahim, W.A.N., Aboul-enein, H.Y.: Theoretical and molecular docking study of ketoconazole on Heptakis (2,3,6-tri-O-methyl)-β-cyclodextrin as chiral selector. Chirality **28**, 209–214 (2016). https://doi.org/10.1002/chir
60. Ibrahim, W.A.W., Arsad, S.R., Maarof, H., Sanagi, M.M., Aboul-Enein, H.Y.: Chiral separation of four stereoisomers of ketoconazole drugs using capillary electrophoresis. Chirality **27**(3), 223–227 (2014). https://doi.org/10.1002/chir
61. Stewart, J.J.P.: Optimization of parameters for semiempirical methods V: modification of NDDO approximations and application to 70 elements. J. Mol. Model. **13**, 1173–1213 (2007). https://doi.org/10.1007/s00894-007-0233-4
62. Karthikeyan, M., Kumar, M.D., Kaniraja, G., Karunakaran, C.: Journal of molecular graphics and modelling theoretical investigations of free energy of binding and chiral recognition studies of (R)- and (S)-noradrenaline towards β-cyclodextrin. J. Mol. Graph Model. **124**, 108552 (2023). https://doi.org/10.1016/j.jmgm.2023.108552